On a Conservative Solution to Checkerboarding: Examining the Discrete Laplacian Kernel Using Mesh Connectivity

J.A. Hopman, F.X. Trias, and J. Rigola

1 Introduction

CFD codes that are used for industrial applications commonly use a collocated grid arrangement to calculate the physical flow variables. When using a central differencing gradient (CDG) to discretise the continuous operators of the Navier-Stokes equations, a wide stencil is obtained for the Laplacian operator. This wide stencil, in turn, leads to a decoupling between odd and even grid points of the pressure field that results from the pressure Poisson equation. This decoupling can lead to non-physical, spurious modes in the solution, a problem commonly known as the checkerboard problem [Ferziger et al., 2002].

Generally, this problem is avoided by using a compact stencil Laplacian. A method to do so was first developed by Rhie and Chow [Rhie and Chow, 1983]. This method solves the problem of decoupled grid points and eliminates the possibility of spurious modes in the pressure field. However, this method introduces nonphysical, numerical dissipation of kinetic energy [Rhie and Chow, 1983, Felten and Lund, 2006]. This dissipation disrupts the delicate interaction between convective transport and physical dissipation, especially at the smallest scales of motion. By doing so, it becomes impossible to capture the essence of turbulence, which is of high importance in accurate DNS simulations [Verstappen and Veldman, 2003]. Moreover, for LES simulations this dissipation was shown to be of the same order of magnitude as the dissipation introduced by the LES model, decreasing the effectiveness of the model [Komen et al., 2021].

Many general purpose codes favour the extra stability that this method offers at the price of a lower accuracy. Unconditional stability, however, can also be achieved by mimicking the underlying symmetry properties of the continuous operators of the Navier-Stokes equations, when discretising them. A method that does this was

J.A. Hopman · F.X. Trias · J. Rigola
Heat and Mass Transfer Technological Center, Technical University of Catalonia, C/Colom 11, 08222 Terrassa, Spain, e-mail: {jannes.hopman,francesc.xavier.trias,joaquim.rigola}@upc.edu

developed for staggered Cartesian grid arrangements by Verstappen and Veldman [Verstappen and Veldman, 2003] and later extended to collocated unstructured grids by Trias *et al.* [Trias et al., 2014]. Since the kinetic energy is conserved and stability is unconditional, using the method of Rhie and Chow comes at a higher price and an alternative method should be sought after. One method mentioned here is the one described by Larsson and Iaccarino [Larsson and Iaccarino, 2010], in which the kernel of the discrete Laplacian operator matrix is determined and used to eliminate the spurious modes. However, on non-Cartesian grids, this method involves performing a singular value decomposition (SVD), for which the computational cost grows exponentially with the number of grid points, as $\mathscr{O}(N_{grid}^3)$, making this method non-viable for industrial applications [Golub and Van Loan, 1996].

In this work, properties of the discrete wide stencil Laplacian, its kernel and the relation to the connectivity of the mesh will be examined. By understanding this relation better, a prediction can be made for a set of vectors that span the nullspace, and by projecting the pressure solution field onto this nullspace, the spurious modes can be eliminated.

2 Relation between the mesh and the kernel

The greatest advantage of the collocated grid formulation is the possibility to extend the solution domain to complex geometries using unstructured meshes. Therefore, the continuous operators will be discretised in a manner that is suitable for unstructured meshes. For these meshes, however, a central node will not necessarily lie between two neighbouring nodes and therefore the CDG is not defined. Here, a discretisation is used that simplifies to the CDG on uniform Cartesian meshes. Moreover, it mimics the property of CDG that gradients at a central node i only depend on values of neighbouring nodes n, i.e.:

$$[\nabla\phi]_i = \sum_n c_n \phi_n \tag{1}$$

where c_n is some coefficient.

Let the discrete wide stencil Laplacian operator be denoted by $L_c = M\Gamma_{cs}^M \Gamma_{sc}^M G$, which follows the discretisation of Trias *et al.* [Trias et al., 2014] and is a chain of operations: (1) face gradient G, (2) midpoint face-to-cell interpolation Γ_{sc}^M, (3) midpoint cell-to-face interpolation Γ_{cs}^M and (4) divergence M. The cell-centered gradient at node i is given by:

$$\begin{aligned}\left[\Gamma_{sc}^M G\phi_c\right]_i &= \frac{1}{2\,[\Omega_c]_i} \sum_{f\in F_f(i)} [\Omega_s]_f \frac{\phi_n - \phi_i}{\delta_{nf}} \mathbf{n}_{if} \\ &= \frac{1}{2\,[\Omega_c]_i} \sum_{f\in F_f(i)} A_f \phi_n \mathbf{n}_{if}\end{aligned} \tag{2}$$

where $\mathbf{n}_{if}$ is the outward-pointing face-normal vector of face f w.r.t. node i, δ_{nf} is the face-normal distance between neighbouring nodes, Ω_s denotes the face volumes, where $[\Omega_s]_f = \delta_{nf} A_f$ with face area A_f, Ω_c denotes the cell volumes and finally $\sum_{f \in F_f(i)}$ denotes a sum over the faces f that constitute cell i. The second line of equation 2 follows from the fact that ϕ_i can be taken out of the summation and the sum of outward-pointing surface normal vectors, $\mathbf{S}_{if} = A_f \mathbf{n}_{if}$, equals zero:

$$\sum_{f \in F_f(i)} \mathbf{S}_{if} = \mathbf{0} \tag{3}$$

Therefore, the value in the central node i does not contribute to the gradient in the central node itself and equation 1 holds. Similarly, the cell-centered divergence at node i is given by:

$$\begin{aligned} [M\Gamma_{cs}\psi_c]_i &= \frac{1}{2} \sum_{f \in F_f(i)} (\psi_i + \psi_n) \cdot \mathbf{n}_{if} A_f \\ &= \frac{1}{2} \sum_{f \in F_f(i)} \psi_n \cdot \mathbf{n}_{if} A_f \end{aligned} \tag{4}$$

Again, the value in the central node i does not contribute to the divergence in the central node itself. L_c is a sequence of both operators connecting nodes i to k if they share a neighbour j, its entries are given by:

$$[L_c]_{i,k} = \sum_j \frac{1}{4\,[\Omega_c]_j} \mathbf{S}_{ij} \cdot \mathbf{S}_{jk} \tag{5}$$

where $\mathbf{S}_{ij}$ is the surface-normal vector, pointing from node i to j. This implies that the Laplacian in node i does not depend on the values in its neighbours j, only on its second neighbours k.

On certain meshes, this can create checkerboard-like patterns. Non-trivial pressure modes can exist on these meshes of which the Laplacian equals zero, i.e. the pressure modes given by a vector in the nullspace of L_c. Several examples of two-dimensional meshes are shown in figure 1, in which cells are coloured the same way if they are connected with non-zero entries in L_c, given by equation 5. Meshes in which the number of faces that meet each other is always even, figure 1(left), show a parity. In this example the nullity of L_c is increased to 2. In the case of Cartesian meshes, figure 1(middle), the dot product in 5 equals zero for diagonal second neighbour pairs, giving rise to a nullity of L_c of $2^{N_{dim}}$, which equals 4 in the two-dimensional example. Finally, meshes in which an uneven number of non-orthogonal faces meet each other, figure 1(right), the disconnection vanishes and the nullity of L_c reduces, in this example to 1.

For the current definition of L_c, the nullity can simply be seen from the connected groups in the mesh. In practice, a nullity higher than 1 will mostly occur in Cartesian meshes, therefore other mesh types are disregarded for now. What remains is to define a set of vectors that span the nullspace of L_c for Cartesian meshes.

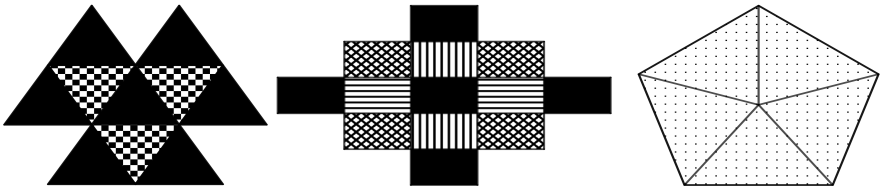

Fig. 1 Several mesh structures showing mesh connectivity. Triangular with parity (left), Cartesian (middle), triangular without parity (right)

To do so, the pressure field $\mathbf{p}_c$ is decomposed into its physical modes, $\mathbf{p}_c^{\oplus}$, and the non-physical modes, $\mathbf{p}_c^{\ominus}$, which lie in the nullspace of L_c: $\mathbf{p}_c = \mathbf{p}_c^{\oplus} + \mathbf{p}_c^{\ominus}$, such that $L_c\mathbf{p}_c = L_c\mathbf{p}_c^{\oplus}$, because $L_c\mathbf{p}_c^{\ominus} = \mathbf{0}_c$. Any $\mathbf{p}_c^{\ominus}$ will then be a linear combination of nullspace spanning vectors. For Cartesian meshes, such a set was given by [Larsson and Iaccarino, 2010], in the two-dimensional example this set is visualised in figure 2 and given by:

$$[\mathbf{p}_c^{\ominus(1)}]_{i,j} = 1, \quad [\mathbf{p}_c^{\ominus(2)}]_{i,j} = (-1)^i, \quad [\mathbf{p}_c^{\ominus(3)}]_{i,j} = (-1)^j, \quad [\mathbf{p}_c^{\ominus(4)}]_{i,j} = (-1)^{i+j} \tag{6}$$

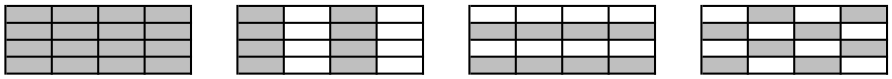

Fig. 2 Visualisation of a set of vectors spanning the nullspace of L_c

The kernel of L_c only depends on the mesh and the choice of interpolator. Therefore, all that remains is to generalise the set of equation 6 to other types of interpolators. Definitions of the most commonly used interpolators, linear and volumetric, are given by:

$$\left[\Gamma_{cs}^{L}\phi\right]_f = \frac{\delta_{nf,n}}{\delta_{nf}}\phi_i + \frac{\delta_{nf,i}}{\delta_{nf}}\phi_n, \quad \left[\Gamma_{cs}^{V}\phi\right]_f = \frac{\delta_{nf,i}}{\delta_{nf}}\phi_i + \frac{\delta_{nf,n}}{\delta_{nf}}\phi_n \tag{7}$$

respectively. Where $\delta_{nf,i}$ and $\delta_{nf,n}$ are the perpendicular distances between face f and centroids i and n respectively, so that:

$$\delta_{nf} = \delta_{nf,i} + \delta_{nf,n} \tag{8}$$

Now it is important to note that, in the symmetry preserving framework, the cell-to-face and face-to-cell interpolators are related to each other by [Trias et al., 2014]:

$$\Gamma_{sc} = \Omega^{-1}\Gamma_{cs}^{T}\Omega_s \tag{9}$$

This leaves only one degree of freedom in L_c, namely the choice of Γ_{cs}.

To find a set of nullspace spanning vectors, the cell-centered gradient, $\Gamma_{sc}G$, is first rewritten to a Gauss gradient form, which is more commonly used in code implementations:

$$[G_G\phi]_i = \frac{1}{[\Omega_c]_i}\sum_{f\in F_f(i)} \mathbf{S}_f\phi_f \tag{10}$$

Next, as an example, the volumetric cell-centered gradient is rewritten to a Gauss Gradient form:

$$\begin{aligned}
\left[\Gamma^V_{sc}G\phi\right]_i &= \left[\Omega^{-1}\Gamma^{V^T}_{cs}\Omega_s G\phi\right]_i && \textit{from eqn. 9}\\
&= \tfrac{1}{[\Omega_c]_i}\textstyle\sum_{f\in F_f(i)}\mathbf{S}_f\delta_{nf}\left(\tfrac{1}{\delta_{nf}}\tfrac{\delta_{nf,i}}{\delta_{nf}}\phi_n - \tfrac{1}{\delta_{nf}}\tfrac{\delta_{nf,i}}{\delta_{nf}}\phi_i\right) && \textit{from eqn. 7}\\
&= \tfrac{1}{[\Omega_c]_i}\textstyle\sum_{f\in F_f(i)}\mathbf{S}_f\left(\tfrac{\delta_{nf,i}}{\delta_{nf}}\phi_n - \left(1-\tfrac{\delta_{nf,f}}{\delta_{nf}}\right)\phi_i\right) && \textit{from eqn. 8}\\
&= \tfrac{1}{[\Omega_c]_i}\textstyle\sum_{f\in F_f(i)}\mathbf{S}_f\left(\tfrac{\delta_{nf,i}}{\delta_{nf}}\phi_n + \tfrac{\delta_{nf,f}}{\delta_{nf}}\phi_i\right) && \textit{from eqn. 3}\\
&= \left[G_G\Pi^L_{cs}\phi\right]_i && \textit{from eqn. 10}
\end{aligned} \tag{11}$$

where in the final step it is simply noticed that the weights are the same as for a scalar linear interpolator, given by Π^L_{cs}. Any cell-centered gradient can be rewritten to a Gauss gradient and a scalar interpolator, by rewriting the interpolation weight of ϕ_i as: $w_{f,i} = 1 - w_{f,n}$. The interpolators considered in this work are rewritten by:

$$\Gamma^M_{sc}G = G_G\Pi^M_{cs}, \qquad \Gamma^L_{sc}G = G_G\Pi^V_{cs}, \qquad \Gamma^V_{sc}G = G_G\Pi^L_{cs} \tag{12}$$

These relations can be used to find the nullspace spanning vectors any Laplacian operator, since we can simply find vectors for which $G_G\Pi_{cs} = \mathbf{0}_c$. Moreover, many codes use linear interpolation for the predictor velocity on the source side of the Poisson equation, combined with a linear interpolation of pressure before taking the Gauss gradient: $L_c = M\Gamma^L_{cs}G_G\Pi^L_{cs} = M\Gamma^L_{cs}\Gamma^V_{sc}G$, which is non-symmetric. This non-symmetry in the operator can disrupt the conservation of physical properties or it may even be the cause of spurious pressure modes to arise in the first place, since the image of L_c and the kernel are not orthogonal if L_c is non-symmetric. To predict a set of nullspace spanning vectors a simple adjustment can be made to the set in equation 6:

$$\begin{aligned}
[\mathbf{p}_c^{\ominus(1)}]_{i,j} &= 1, & [\mathbf{p}_c^{\ominus(2)}]_{i,j} &= (-1)^i(\Delta x_i)^\alpha\\
[\mathbf{p}_c^{\ominus(3)}]_{i,j} &= (-1)^j(\Delta y_j)^\alpha, & [\mathbf{p}_c^{\ominus(4)}]_{i,j} &= (-1)^{i+j}(\Delta x_i\Delta y_j)^\alpha
\end{aligned} \tag{13}$$

where $\alpha = [-1,0,1]$ for volumetric, midpoint and linear interpolations respectively. It can be easily verified that these vectors lie in the nullspace of their respective L_c. Moreover, although the vectors are not necessarily orthogonal, they are linearly independent and therefore span the nullspace of L_c. This is required since $\mathbf{p}_c$ is projected onto the nullspace and the result is subsequently subtracted to obtain $\mathbf{p}_c^{\oplus}$.

3 Conslusions

It was shown in this work that there is a strong relation between the nullity of L_c and the used mesh. Moreover, it was shown that the nullity will in practice most often be 1 for unstructured meshes, in which case the nullspace consists of the constant vector. For Cartesian meshes the nullity is known and a set of nullspace spanning vectors was derived for the most commonly used interpolators in the Laplace operator. Thereby in a strict mathematical sense, the spurious modes can effectively be filtered in almost any case. This leads to the question if the wide stenciled Laplacian can also give rise to decoupled pressure modes that do not strictly lie in its nullspace, and if they can be filtered easily as well. These questions will be addressed in future work.

Acknowledgements This work is supported by the FusionCAT project (001-P-001722) co-financed by the European Union Regional Development Fund within the framework of the ERDF Operational Program of Catalonia 2014-2020 with a grant of 50% of total cost eligible. The work is part of the RETOtwin project (PDC2021-120970-I00) of *Ministerio de Economía y Competitividad*, Spain. J.A.H. is supported by the predoctoral grant FI 2022 (2022 FI_B1 00204) of the *Catalan Agency for Management of University and Research Grants (AGAUR).*

References

[Felten and Lund, 2006] Felten, F. N., & Lund, T. S. (2006). Kinetic energy conservation issues associated with the collocated mesh scheme for incompressible flow. Journal of Computational Physics, 215(2), 465-484.

[Ferziger et al., 2002] Ferziger, J. H., Perić, M., & Street, R. L. (2002). Computational methods for fluid dynamics (Vol. 3, pp. 196-200). Berlin: springer.

[Golub and Van Loan, 1996] Golub, G. H., & Van Loan, C. F. (1996). Matrix computations, johns hopkins u. Math. Sci., Johns Hopkins University Press, Baltimore, MD.

[Komen et al., 2021] Komen, E. M., Hopman, J. A., Frederix, E. M. A., Trias, F. X., & Verstappen, R. W. (2021). A symmetry-preserving second-order time-accurate PISO-based method. Computers & Fluids, 225, 104979.

[Larsson and Iaccarino, 2010] Larsson, J., & Iaccarino, G. (2010). A co-located incompressible Navier-Stokes solver with exact mass, momentum and kinetic energy conservation in the inviscid limit. Journal of Computational Physics, 229(12), 4425-4430.

[Rhie and Chow, 1983] Rhie, C. M., & Chow, W. L. (1983). Numerical study of the turbulent flow past an airfoil with trailing edge separation. AIAA journal, 21(11), 1525-1532.

[Trias et al., 2014] Trias, F. X., Lehmkuhl, O., Oliva, A., Pérez-Segarra, C. D., & Verstappen, R. W. C. P. (2014). Symmetry-preserving discretization of Navier–Stokes equations on collocated unstructured grids. Journal of Computational Physics, 258, 246-267.

[Verstappen and Veldman, 2003] Verstappen, R. W. C. P., & Veldman, A. E. P. (2003). Symmetry-preserving discretization of turbulent flow. Journal of Computational Physics, 187(1), 343-368.